Asphaltene Fractionation Based on Adsorption onto Calcium Carbonate:

Part 2. Self-association and Aggregation properties

Sreedhar Subramanian[1]*, Geir Humborstad Sørland[2], Sébastien Simon[1], Zhenghe Xu[3] and Johan Sjöblom[1]

[1]Ugelstad Laboratory, Department of Chemical Engineering, Norwegian University of Science and Technology (NTNU), N-7491 Trondheim, Norway.

[2]Anvendt Teknologi AS, Munkvollveien 56, 7022 Trondheim, Norway.

[3]Department of Chemical and Material Engineering, University of Alberta, Edmonton, Alberta T6G 1H9, Canada.

ABSTRACT

The self-association and aggregation properties of asphaltene sub-fractions obtained by adsorption onto $CaCO_3$ (doi:10.1016/j.colsurfa.2016.02.011) were investigated using a combination of near infrared spectroscopy, isothermal titration calorimetry (ITC) and diffusion-ordered 2D NMR spectroscopy (DOSY). Three asphaltenes sub-fractions were prepared: the *bulk* fraction that stayed in the bulk solution (i.e., did not adsorb on $CaCO_3$), the *adsorbed* fraction that was obtained by desorption of asphaltenes adsorbed on $CaCO_3$ using tetrahydrofuran, and the *irreversibly-adsorbed* fraction that was obtained after dissolution of $CaCO_3$. The *irreversibly-adsorbed* asphaltene sub-fraction, which contained a higher content of carbonyl, carboxylic acid or derivative groups was found to have a significantly higher tendency to self-associate and to form larger aggregates than other fractions. In addition, the properties of above asphaltene fractions were compared with fractions obtained by stepwise precipitation using various n-hexane/crude oil ratios to study the influence of fractionation procedure. The *irreversibly-adsorbed* asphaltenes exhibited several similarities in properties with the fraction precipitating first from stepwise precipitation procedure (named as

asphaltene *3.5V*) including lower flocculation onset, higher tendency to self-associate (based on ITC) and a greater ability to adsorb onto stainless steel (based in QCM-D measurements). However, the size of aggregates determined by NMR differed, with the *irreversibly-adsorbed* asphaltenes forming aggregates of larger aggregate size (11.3 Å) than compared to asphaltene 3.5V fractions (7.2 Å). In conclusion, our investigations indicate that the asphaltene precipitation tendency depends on both the aromaticity and polarity of asphaltene fractions, and some of the asphaltene sub-fractions present different properties than the *whole* (or unfractionated) asphaltene fraction.

KEYWORDS

Asphaltene fractionation; Isothermal Titration Calorimetry (ITC); DOSY NMR; NIR; FTIR

1.	INTRODUCTION

Asphaltenes are defined as a solubility class: insoluble in n-alkanes (n-pentane or n-heptane) but soluble in aromatic solvents like toluene or benzene[1]. The definition of asphaltenes as a solubility class leads to presence of thousands of molecules with broad molecular weight distribution being classified under asphaltene fraction[2]. The average molecular weight of asphaltenes is considered to be around 750 g/mol with a majority of molecules in the range 500 – 1000 g/mol. Asphaltenes are characterized by the presence of polycyclic aromatic hydrocarbons (PAH) with fused rings, aliphatic side chains and heteroatoms. Different models have been proposed to represent "average" asphaltene chemical structure like "island/continental architecture" with a single PAH or "archipelago architecture" with several PAHs connected by alkyl chains per asphaltene molecule[3]. Recent studies suggest the dominance of island architecture in the asphaltenes[4], and that the polyaromatic core consists of roughly 6-7 fused rings on an average[5, 6]. The presences of polyaromatic core in asphaltenes results in interaction among asphaltene molecules through π-π stacking, and in combination with interactions between polar groups induce the formation of nanoaggregates. According to the Yen-Mullins model, the nanoaggregates typically consist of up to 6 asphaltene molecules, and these nanoaggregates in turn can form clusters with aggregation numbers of ~8[7]. In case of asphaltenes with island architecture, the aliphatic side chains surrounding the large PAH cause steric hindrance and limit the number of asphaltene molecules in nanoaggregate[8, 9]. Asphaltenes with archipelago architecture however tend to form complex aggregates due to the presence of bridging or 'tangling' chains between PAHs[8]. In addition to π-π stacking, asphaltene molecules can associate through acid-base interactions, hydrogen bonding between functional groups and charge transfer interaction[10, 11].

The self-association and aggregation of asphaltenes is believed to be the first step involved during the process of asphaltene precipitation from crude oil[12]. Unstable crudes generally consist of asphaltenes with low H/C ratio and high aromaticity[13]. Several techniques have been employed to study the asphaltene aggregation including near-infrared (NIR) spectroscopy[14, 15], small angle neutron scattering (SANS)[11, 16, 17], vapor pressure osmometry (VPO)[18, 19], surface/interfacial tension measurements[19, 20], isothermal titration calorimetry (ITC)[21-23], nuclear magnetic resonance (NMR) spectroscopy[12] and diffusion-ordered two-dimensional (2D) NMR spectroscopy (DOSY)[24-27]. Attempts have also been made to fractionate asphaltenes into sub-fractions of reduced complexity and to identify fractions responsible for precipitation problems[11]. The least soluble asphaltene fraction has been found to contain more polar species, form larger aggregates and also contribute significantly to asphaltene aggregation[11, 28].

Isothermal titration calorimeter (ITC) is a useful tool to determine the thermodynamics of interaction between molecules. The experimental heats obtained by ITC for asphaltenes self-association are comparable to those obtained by molecular simulations, thereby indicating the applicability of ITC to study the interaction involving asphaltenes[29]. The technique has also been used to study the interaction between asphaltenes and resins[30], tetrameric acids[31], model inhibitors like nonylphenol[22, 32] and dodecylbenzene sulfonic acid[22]. The study of asphaltene self-association using ITC has been carried out mainly in good solvents like toluene[21] or xylene[22]. The tendency of asphaltenes to self-associate and form nanoaggregates even in good solvents have been reported[33]. The self-association of asphaltene molecules is believed to proceed via a step-wise aggregation mechanism in disagreement with the Yen-Mullins model presented above, and the enthalpy change (ΔH)

associated with aggregate formation is in the range of -2 to -7 kJ/mol[34]. In addition, the sub-fractions of asphaltenes were also found to show differences in enthalpic heats[34].

Recently, pulsed field gradient spin echo (PFGSE) Nuclear Magnetic Resonance (NMR) and diffusion-ordered two-dimensional (2D) NMR spectroscopy (DOSY) have been employed for physio-chemical characterization of asphaltenes[12, 24-27, 35, 36]. Both techniques measure the diffusion coefficients of asphaltene molecules or aggregates as well as the solvent. The asphaltene sizes (hydrodynamic radius) can then be extracted from diffusional measurements. The DOSY NMR is a derivate of PFGSE NMR, and offers the advantage of obtaining a NMR chemical shift on one axis and the diffusion co-efficient on the other[37]. For asphaltenes obtained from vacuum residue from a Venezuelen crude oil, Östlund et al.[35] measured a diffusion co-efficient of 2.2 x 10^{-10} m^2/s for asphaltenes at infinite dilution and also proposed that the asphaltenes have a disc like shape. It has been observed that the diffusion co-efficient of asphaltenes tend to decrease beyond a certain concentration thereby indicating the onset of aggregation[26, 27, 36]. Durrand et al.[26] observed that the diffusion co-efficients of asphaltenes in toluene at infinite dilution were different for asphaltenes with continental and archipelago type structures. Asphaltenes in Maya and Buzurgan crude oils exhibited higher diffusion co-efficients and formed nano-aggregates with a hydrodynamic radius of ∼15.6Å, and was hence considered to consist of predominantly continental type structure, while the asphaltenes in Athabasca crude oil had a lower diffusion co-efficient and formed nano-aggregates of bigger radius (∼19Å), and therefore considered to have predominantly archipelago type structure[26]. Similarly, Lisitza el al.[27] observed that asphaltenes from Kuwaiti UG8 crude oil formed nano-aggregates of radius ∼12Å.

In our earlier work[38], asphaltenes from Norwegian Continental Shelf were fractionated based on adsorption onto calcium carbonate. Three asphaltenes sub-fractions were prepared: the *bulk* fraction that stayed in the bulk solution (i.e., did not adsorb on $CaCO_3$), the *adsorbed* fraction that was obtained by desorption of asphaltenes adsorbed on $CaCO_3$ using tetrahydrofuran, and the *irreversibly-adsorbed* fraction that was obtained after dissolution of $CaCO_3$. The asphaltenes fractions were characterized by elemental analysis and Fourier Transform Infrared Spectroscopy (FTIR). The ability of different asphaltene fractions to adsorb onto stainless steel surface was then studied using QCM. The present paper focuses on investigation of aggregation properties of asphaltenes based on Near-Infrared Spectroscopy (NIR), Isothermal Titration Calorimetry (ITC) and DOSY NMR techniques. A new procedure to fractionate asphaltenes based on stepwise precipitation from crude oil is developed. The characteristics and properties of asphatene fractions obtained by stepwise precipitated technique are studied, and an attempt is finally made to identify the similarities and differences between asphaltenes sub-fractions obtained from the two fractionation methods.

2.   EXPERIMENTAL METHODS

2.1.   CHEMICALS

A chemical free crude oil from Norwegian Continental Shelf was used for asphaltene extraction. The characteristics of the crude oil used can be found in our earlier publication[38]. N-hexane (VWR, >97%) was used for extracting asphaltenes from crude. Fractionation of asphaltenes was carried out using precipitated $CaCO_3$ (Specialty Minerals, US), anhydrous toluene (Sigma Aldrich, 99.8%), anhydrous tetrahydrofuran (VWR, >99.7), Chloroform (Merck, >97%), hydrochloric acid (Merck, 37%) and milli-Q water. The acidic polyaromatic model compound *N*-(1-undecyldodecyl)-*N′*-(5-carboxylicpentyl)perylene-

3,4,9,10-tetracarboxylbisimide (C5PeC11)was synthesized by following the procedure described in Pradilla et al.[39] The solvent used for ITC experiment was xylene (VWR, >98.5%), while the NMR experiments were performed with deuterated toluene (Sigma Aldrich, 99.6 atom% D).

2.2. Asphaltene extraction

The crude oil was conditioned at 60°C for two hours before sampling. The crude oil was diluted with an excess of n-hexane in the ratio 1:40 (w/v). The mixture was stirred overnight at room temperature (22°C) and filtered using a Millipore 0.45µm filter. The precipitated asphaltenes was washed with n-hexane until the filtrate obtained was colorless. The asphaltenes were dried under nitrogen purge at room temperature. The asphaltenes obtained was called as *whole* asphaltenes.

2.3. Asphaltene fractionation

2.3.1. Fractionation based on adsorption onto $CaCO_3$

The detailed procedure for fractionation of *whole* asphaltenes based on adsorption onto $CaCO_3$ is described in an earlier work[38]. In short, *whole* asphaltenes were initially dissolved in toluene and then $CaCO_3$ was added to it. The mixture was stirred at room temperature for 24 hours before centrifuging the mixture at 4000 rpm for 20 min. The supernatant was concentrated to dryness and the asphaltenes obtained was called as *bulk* asphaltenes. THF was added to the $CaCO_3$ (remaining after centrifugation, containing some asphaltenes adsorbed to it) and the mixture was stirred at 45°C for 24 hours. The mixture was then centrifuged at 4000 rpm for 20 min. The supernatant was concentrated to dryness and the asphaltenes obtained was called as *adsorbed* asphaltenes. An equivolume mixture of $CHCl_3$-THF was added to the remaining $CaCO_3$ (which contained asphaltenes strongly

adsorbed on it), followed by addition of 4N HCl solution and stirring for 3-4 hours at room temperature. The organic and aqueous layers were then separated. The organic layer was washed with water and concentrated. The asphaltenes obtained was called as *irreversibly-adsorbed* asphaltenes. It must be noted that the final drying of all asphaltene fractions (*bulk*, *adsorbed* and *irreversibly-adsorbed*) was done on a block heater (GRANT UBR) set at 70°C under a stream of nitrogen.

2.3.2. Fractionation based on bulk precipitation

The crude oil was initially conditioned for 2 hours at 60°C. 20g of crude oil was then sampled and transferred into a 1 liter flask. The fractionation procedure followed is shown in figure 1.
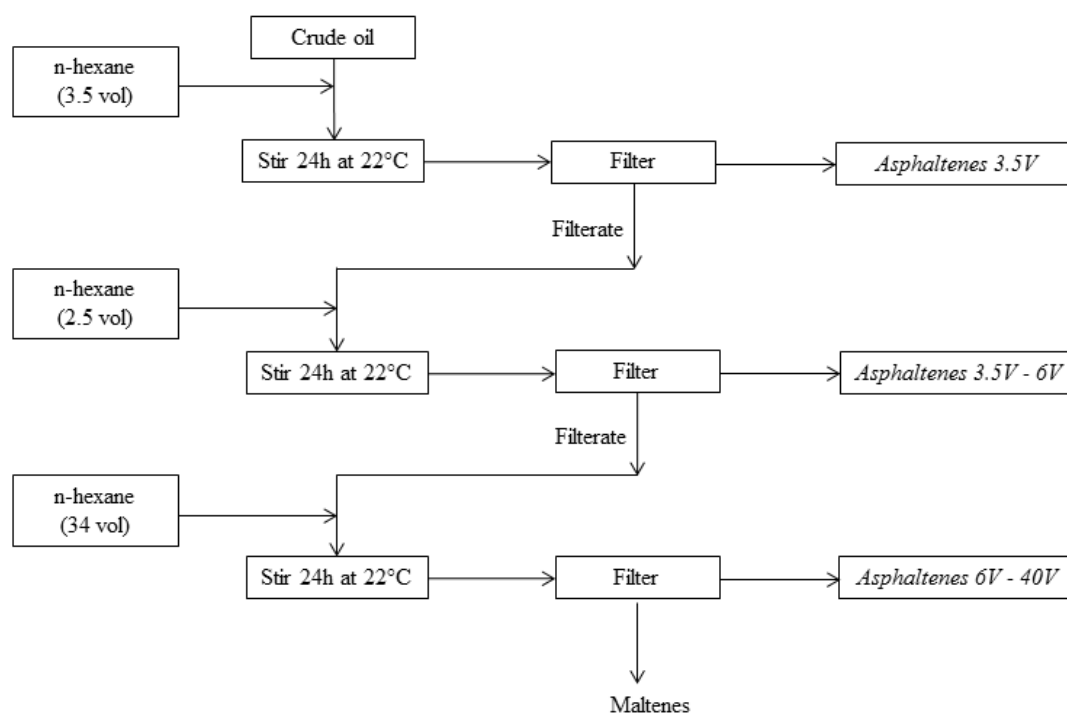

Figure 1: Asphaltene fractionation based on bulk precipitation using n-hexane. Note that the n-hexane volume (vol) refers to volume per gram of crude oil.

70ml (or 3.5vol/g of crude oil) of n-hexane was added to the flask containing 20g of crude oil, and the mixture was allowed to stir for 24 hours at 22°C. The oil mixture was filtered using Millipore 0.45µm filter paper and the asphaltenes were washed with 50ml of n-hexane. The asphaltenes obtained (known as *asphaltenes 3.5V*) were dried under nitrogen at room temperature. The filtrate was diluted upto 6 volumes of n-hexane and was allowed to stir for 24 hours at 22°C. The oil mixture was filtered using Millipore 0.45µm filter paper and the asphaltenes were washed with 50ml of n-hexane. The asphaltenes obtained (known as *asphaltenes 3.5V-6V*) were dried under nitrogen at room temperature. The filtrate was then diluted upto 40 volumes of n-hexane and allowed to stir for further 24 hours at 22°C. The oil mixture was once again filtered using Millipore 0.45µm filter paper and the asphaltenes were washed with 50ml of n-hexane. The asphaltenes obtained (known as *asphaltenes 6V-40V*) were dried under nitrogen at room temperature. It must be noted that the evaporation of n-hexane during vacuum filtration was compensated during all the steps by weighing the filtrate.

2.4. Elemental Analysis

The elemental composition (C, H, N, O, S) and metal content (Fe, Ni, V, Ca, Na, K) of the crude oil and the asphaltene fractions were determined by Laboratory SGS Multilab (Evry, France) by thermal conductivity measurements for C, H and N, infrared measurements for O and S, and ICP-AE measurements after mineralization in bomb Milestone by microwave for metal content. The relative uncertainties in measurement of metal content are as follows: Fe ($\pm$ 5%), Ni ($\pm$10%), V ($\pm$7%), Ca ($\pm$10%), Na ($\pm$15%) and K ($\pm$10%).

2.5. Fourier Transform Infrared Spectroscopy (FTIR)

A Tensor 27 spectrometer (Bruker Optics) equipped with a Bruker Golden Gate diamond Attenuated Total Reflection (ATR) cell was used to record the FTIR spectra of the samples in the spectral range 4000 to 600 cm^{-1}, with 4 cm^{-1} resolution. 10 g/L solutions of asphaltene in CH$_2$Cl$_2$ were prepared, and 3-5 drops of sample was placed on the cell. The measurements were done after the solvent had completely evaporated.

2.6.   Near Infrared Spectroscopy (NIR)

A Multi-Purpose Analyzer (MPA) from Bruker Optics was used for spectral characterization of the samples in the near infrared range 1100 to 2500 nm. Asphaltene solutions of concentration 10 g/L was initially prepared by adding 9.1g of toluene to 105 mg of asphaltenes. The asphaltene solution was sonicated for 30 min and the dissolution was checked visually by observing a drop of solution under a microscope for presence of particles. The asphaltene solution of 2 g/L concentration at different toluene/n-hexane ratios was prepared by diluting the 10 g/L solution. The volume fraction of n-hexane in the solution was varied from 0 to 0.8.

2.7.   Isothermal Titration Calorimetry (ITC)

The calorimetric investigations were carried out using NANO ITC Standard volume from TA instruments. An internal electronic calibration device was first used to calibrate the heat signal. Thereafter, the heat of reaction between Trizma and HCl was measured, and compared with the literature. For the experiment, the reference cell was initially filled with sonicated xylene. 10 g/L solution of asphaltenes in xylene was prepared by dissolving asphaltene in xylene followed by sonication for 30 min. The asphaltene solution was then loaded into 250μL syringe and placed in the burette connected to the sample cell in calorimeter. Before starting the titration experiment, the stirrer was set at 250 rpm and the calorimeter was

equilibrated (i.e., baseline drift < 0.1 µW over 20 min). A 300s baseline was collected before injecting the 10 g/L asphaltene solution sequentially in steps of 10 µL. The injection interval was 400s. A 300s baseline was also collected at the end of the experiment. All the experiments were carried out at 25°C.

2.8.   [1]H Diffusion-ordered Spectroscopy (DOSY) Nuclear Magnetic Resonance (NMR)

Diffusion-ordered Spectroscopy (DOSY) provides a tool that correlates the resonance frequency with the molecular mobility of the sample[40, 41]. This technique allows us to determine the diffusion co-efficient of species in solution.
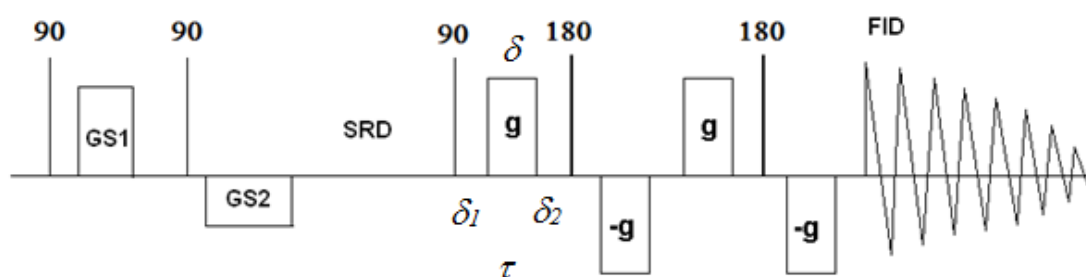

Figure 2: The rapid DOSY experiment

Figure 2 shows the ordinary DOSY sequence combined with the Spoiler Recovery (SR) approach[42]. The diffusion and longitudinal relaxation time measurements are traditionally performed by allowing the magnetization to recover back to thermal equilibrium after application of radio frequency (RF) and magnetic gradient pulses. However, this approach is time consuming. Hence a combination of two 90° RF pulses and two magnetic gradient pulses (GS1 and GS2) of opposite polarity are applied (known as the spoiler recovery sequence). The application of the SR approach in high-resolution experiments provides the

possibility of acquiring data from components of low-abundance within a reasonable measurement time of one hour.

The attenuation of the Fourier transformed FID for a multi exponential system at a given frequency, ν is written as

$$I_{(\nu)} = I_{0(\nu)} \sum_i \rho_i \left(1 - exp^{\frac{SRD^i}{T_1^i}}\right) exp^{-\gamma^2 4g^2 \delta^2 D^i \left(\frac{3}{2}\tau - \frac{\delta}{6}\right) - \frac{4\tau}{T_2^i}} \tag{1}$$

γ is the gyromagnetic ratio, ρ_i is the weighting factor of region i, D^i is the diffusion coefficient, T_1^i is the longitudinal relaxation time, g is the applied gradient strength, *GS1* and *GS2* are the spoiler gradient pulses, δ_1, δ_2, δ and τ are time duration parameters, and the SRD is the spoiler recovery delay[42].

Since the recycle delay can be set to practically zero and the SR can be set to T_1, several more scans may be accumulated within the same acquisition time as the traditional method of applying a recycle delay of 5 times T_1.[42] By fixing spoiler recovery delay (SRD) and incrementing the gradient strength only, a set of FID's (free induction delay) as a function of gradient strength is produced. After a Fourier transform (FT) of the FID, the spectra can be subjected to a one dimensional inverse Laplace routine, resulting in a distribution of diffusion coefficients for each frequency point in the spectra. From equation 1, it is seen that a change in SRD will lead to different contributions from components with different T_1 relaxation time. This can be used for solvent suppression, as one usually wants to study macromolecules with short T_1's dissolved in a solvent having a much longer T_1.

For the experiments, the asphaltene solutions were prepared by dissolving the asphaltenes fractions in toluene-D_8 at a concentration of 0.1 wt%. The samples were then filled into 3 mm

NMR tubes and measured at 25°C using a 600 MHz Bruker spectrometer equipped with a cryoprobe. With this probe we had access to only 50 Gauss/cm, so in order to have proper attenuation the 13-interval PFGSTE sequence[43] was applied with sinusoidal gradient pulse lengths of 3 ms and a z-storage interval of 300 ms. With the sample size applied, there were no significant temperature gradients over the sample, and it was not necessary to apply convection compensated DOSY sequences[44].

2.9. Quartz Crystal Microbalance (QCM-D)

The adsorption of asphaltenes onto quartz crystal coated with stainless steel (supplied by Biolin scientific) was measured using a quartz crystal microbalance with dissipation (QCM-D). The apparatus used was a single sensor microbalance system Q-sense E1 from Biolin Scientific (Sweden). Prior to the start of experiment, the crystals were cleaned according to the following protocol: the crystal was immersed in 1% hellmanex solution in water for at least 1 hour followed by washing with purified water, sonication in ethanol for 10 min, drying with N_2 and finally treated in UV chamber for 15 min.

QCM adsorption experiments were performed with the following procedure: xylene was initially passed through the chamber containing crystal at 20°C to obtain a baseline. The baseline was considered to be stable if the frequency change was less than ±1 Hz for 10 min. Solutions of asphaltene in xylene were then injected into the chamber in a stepwise manner using a pump (flow rate = 750 µL/min). Sample injection time was 10 min followed by a waiting time of 5 min before the next sample injection was performed. Desorption study was done by injecting xylene after passing the most concentrated asphaltene solution. The QCM experiments were repeated at least twice for each measurement.

The QCM-D operates based on the property of piezoelectricity. The piezoelectric quartz crystal coated with stainless steel is located between the two metal electrodes. By applying an AC voltage across the electrodes, the crystal is excited to oscillate. The frequency of oscillation is dependent on the mass adsorbed onto the surface of the crystal. The relationship between the change in frequency (Δf) due to the mass adsorbed (Δm) was established by Sauerbrey[45] as (equation 2)

$$\Delta m = -\frac{\rho_q t_q}{f_o n}\Delta f = -\frac{\rho_q v_q}{2f_o^2 n}\Delta f = -\frac{C}{n}\Delta f \qquad (2)$$

Where ρ_q (=2648 kg/m^3) and t_q (=0.3 mm) are the mass density and thickness of the crystal, v_q (=3340 m/s) is shear wave velocity in quartz, f_o (= 5 MHz) is the fundamental frequency of crystal and n is the overtone number. The constant C equals 0.177 mg/m^{2}Hz. In the present study, the values obtained for the 5th overtone are reported since the dissipation change corresponding to 3rd overtone was earlier found to be sensitive to flow changes[38]. The Sauerbrey equation is valid only when the mass adsorbed is evenly distributed on the surface, Δm is smaller than the mass of the crystal and the adsorbed mass is rigidly attached to the surface[45].

The change in dissipation due to adsorption is given by the relationship[46]

$$D = \frac{E_{disspiated}}{2\pi E_{stored}} \qquad (3)$$

Where D is the dissipation factor, $E_{disspiated}$ is the energy dissipated during one period of oscillation and E_{stored} is the energy stored in the oscillating system. In the case of formation of viscoelastic films on the surface, the Sauerbrey's relationship (equation 1) is no longer valid.

3.   RESULTS AND DISCUSSION

3.1.   Fractional yields

Fractionation of whole asphaltenes based on adsorption onto CaCO$_3$ resulted in the following fractional yields as reported in an earlier study[38]: *bulk* asphaltenes (49 wt%), *adsorbed* asphaltenes (29.5 wt%) and *irreversibly-adsorbed* asphaltenes (20.5 wt%). The overall recovery of asphaltenes after fractionation was ∼99 wt%.

A calibration curve was necessary to determine the conditions necessary to develop method for stepwise precipitation of asphaltenes by diluting crude oil with n-hexane. Hence, samples of crude oil (10g each) were diluted with different volumes of n-hexane and the amount of asphaltenes precipitated was measured. The percentage of total asphaltene precipitated at different volumes of n-hexane dilution of crude oil is calculated based on the following equation 4.

$$Percentage\ of\ total\ asphaltenes\ precipitated\ (mass\%) = \frac{m_v}{m_{40}} \times 100 \quad (4)$$

Where m_v = mass of asphaltenes precipitated on dilution with v volumes of n-hexane (i.e., ml of n-hexane/g of crude oil) and m_{40} = mass of asphaltenes precipitated on dilution with 40 volumes of n-hexane. The experiments were repeated twice to check for reproducibility.
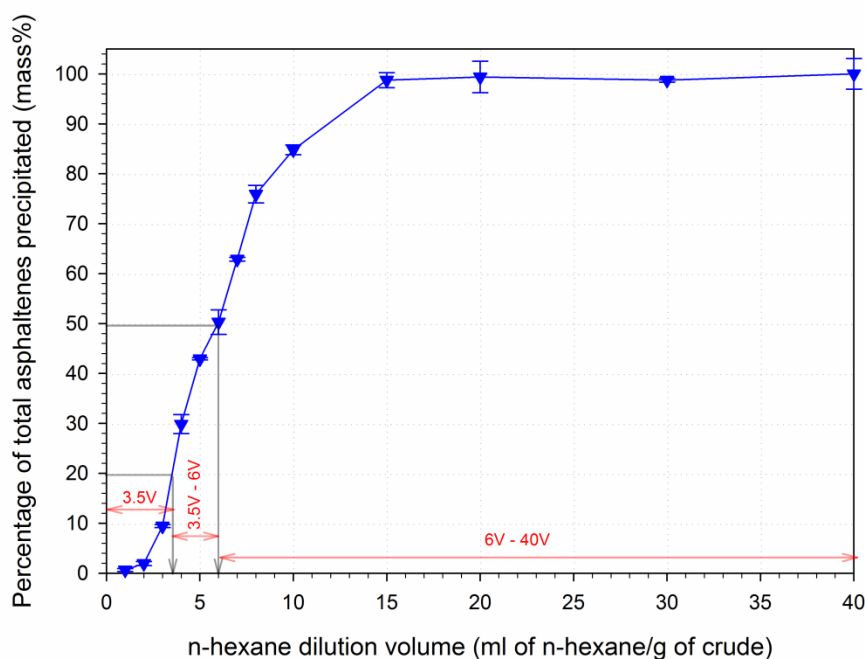
Figure 3: Calibration curve for crude oil dilution with n-hexane based on 2 independent

experiments.

Figure 3 shows the percentage of asphaltenes precipitated at different volumes of n-hexane

dilution. Our aim was to separate asphaltenes from crude oil into 3 fractions of yields 20

wt%, 30 wt% and 50 wt% (i.e., similar to yields obtained for $CaCO_3$ adsorption method). It

can be observed that the first 20 wt% of asphaltenes present in crude precipitates on addition

of ~3.5 volumes of n-hexane to crude oil, the next 30 wt% of asphaltenes precipitates on

addition of further 2.5 volumes of n-hexane and the remaining 50 wt% precipitates on

addition of further 34 volumes of n-hexane. Hence the above conditions were chosen to

fractionate asphaltenes for further study as shown earlier in figure 1.

The yields of different asphaltene fractions (*3.5V*, *3.5V-6V* and *6V-40V*) obtained from 20g of

crude oil based on 5 experiments are given in table 1. The average total recovery of

asphaltenes was around 0.53g from a batch of 20g crude oil, and the recovered asphaltene

amount represents approximately 2.66 wt% of the crude oil. This amount is similar to the

asphaltene content (2.5 wt%) in crude oil based on SARA analysis.[38] Thus all the asphaltenes have been recovered from the crude oil. It can be observed that the percentage yields of fractions *3.5V* and *3.5V-6V* are slightly higher than expected from figure 1, while the percentage yield of fraction *6V-40V* is lower.

Asphaltenes fraction	Yield (g)	Yield (wt %)
3.5V	0.145 ± 0.006	27.4 ± 0.8
3.5V-6V	0.172 ± 0.001	32.3 ± 0.9
6V-40V	0.214 ± 0.012	40.3 ± 1.2
Total	0.531 ± 0.015	~ 100

Table 1: Yield of asphaltene fractions obtained by n-hexane dilution of crude oil on average of 5 independent experiments.

3.2.   Composition

3.2.1. Elemental Analysis

The elemental analysis of asphaltene fractions obtained based on stepwise precipitation using n-hexane dilution of crude is given in table 2. The H/C ratio of the asphaltene fractions (*3.5V, 3.5V-6V, 6V-40V*) varies only over a narrow range (1.13 – 1.16), thereby indicating that the fractions do not show appreciable difference in their aromaticity. The sulfur content in the sub-fractions is evenly distributed. The nitrogen content in asphaltene *3.5V* sub-fraction was however found to be slightly lower than the fractions *3.5V-6V* and *6V-40V*. Variation in oxygen content was however observed among the fractions, with the asphaltene fraction *3.5V* showing a significantly higher presence of O atoms (around 50-60% relative difference) compared to the other two fractions (*3.5V-6V* and *6V-40V*). A similar stepwise fractionation of crude oils by Fossen et al. [47]using n-pentane as precipitant showed an increase in oxygen

content in the first precipitating asphaltene fraction for one of the North Sea Crude oil. The first precipitating asphaltene fractions from two other crude oils they studied did not exhibit similar increase in oxygen content, which could be attributed to a less efficient fractionation of asphaltenes. In comparison, the asphaltenes fractions obtained based on adsorption onto CaCO$_3$ showed more variation with the *irreversibly- adsorbed* fraction exhibiting a slightly higher aliphatic character and also a higher concentration of oxygen[38].

The mass balance of the elements was calculated based from the following equation:

$$\% \, loss \, (or) gain = \frac{f_{3.5V}X_{3.5V} + f_{3.5V-6V}X_{3.5V-6V} + f_{6V-40V}X_{6V-40V}}{X_{whole}} \quad (5)$$

Where, $f_{3.5V}$, $f_{3.5V-6V}$ and f_{6V-40V} refer to the fractional yield of asphaltene fractions *3.5V*, *3.5V - 6V* and *6V – 40V* respectively. X_{whole}, $X_{3.5V}$, $X_{3.5V-6V}$ and X_{6V-40V} refer to the weight percentage (%) of corresponding element in *whole*, *3.5V*, *3.5V - 6V* and *6V - 40V* asphaltene fractions respectively.

| Element | Crude oil | Asphaltenes | | | | %loss or %gain |
		Whole	*3.5V*	*3.5V-6V*	*6V-40V*	
C (wt%)	86.90	85.6	82.3	86.1	86.2	-0.6
H (wt%)	11.67	8.17	7.95	8.21	8.16	-0.6
N (wt%)	0.28	1.32	1.27	1.36	1.35	+0.9
O (wt%)	0.46	1.85	2.84	1.73	1.79	+11.3
S (wt%)	0.87	1.96	2.09	2.13	2.12	+7.9
Total (wt%)	100.18	98.90	96.45	99.53	99.62	-
H/C ratio (-)	1.610	1.145	1.159	1.144	1.136	-

Table 2: Elemental analysis of asphaltene fractions obtained by step-wise precipitation procedure. The mass balance of elements is indicated as % loss (negative) or % gain (positive).

From table 2, it can be observed that there is good mass balance for the elements C, H and N. It must however be noted that the recovery of elemental mass balance for asphaltene 3.5V fraction is slightly lower (around 96.5%), which is consistent with the presence of higher metal content in this sub-fraction (table 3). There is however a marginal gain in oxygen (+11.3 wt%) and sulfur (+7.9 wt%) contents. The oxygen gain is most likely due to uncertainties in measurement and possibility of slight oxidation.

The metal content in different asphaltene sub-fractions is presented in table 3. The asphaltene fraction *3.5V* contains a very high Fe content. The amount of V and Ni is similar in various sub-fractions (*3.5V, 3.5V-6V, 6V-40V*), thereby indicating that there is no tendency for these two metals to be concentrated in any particular asphaltene sub-fraction. However, the whole asphaltenes contain slightly higher Ni and V content than any of the sub-fractions. We suspect that this discrepancy may have been due to sampling. Similarly, the content of calcium and sodium in asphaltene *3.5V* sub-fraction is significantly higher (>10 times) than compared to the fractions *3.5V-6V* and *6V-40V*. This could be attributed to the presence of calcium and sodium salts dissolved in water. The crude oil used for the study has 0.11 wt% water content. The coalescence of water droplets present in crude during the first filtration step (to obtain the *3.5V* fraction) may have most likely resulted in the precipitation of the water soluble inorganic salts along with the less soluble asphaltene fraction.

Element	Crude oil	Asphaltenes				%loss or %gain
		Whole	*3.5V*	*3.5V-6V*	*6V-40V*	
Fe (ppm)	6	96	219	<30	57	< -3.5
V (ppm)	17	256	190	185	178	-28.3
Ni (ppm)	6	77	61	50	58	-27.0
Ca (ppm)	120	1402	3694	225	401	-11.1
Na (ppm)	<50	641	3000	<250	<250	> +30.0
K (ppm)	<50	<130	<250	<250	<250	-

Table 3: Metal content in asphaltene fractions obtained by step-wise precipitation procedure.

The mass balance of elements is indicated as % loss (negative) or % gain (positive).

3.2.2. FTIR Spectroscopy

The FTIR spectroscopy of asphaltene fractions obtained by stepwise precipitation is shown in figure 4. The spectra obtained were baseline corrected by subtracting the values in spectra with the absorbance value at 600 cm^{-1}. The baseline corrected spectra was then normalized by dividing the values in spectra by the highest absorbance value. The spectra are divided into two regions: (a) 3200 - 2600 cm^{-1} and (b) 2000 - 600 cm^{-1}.
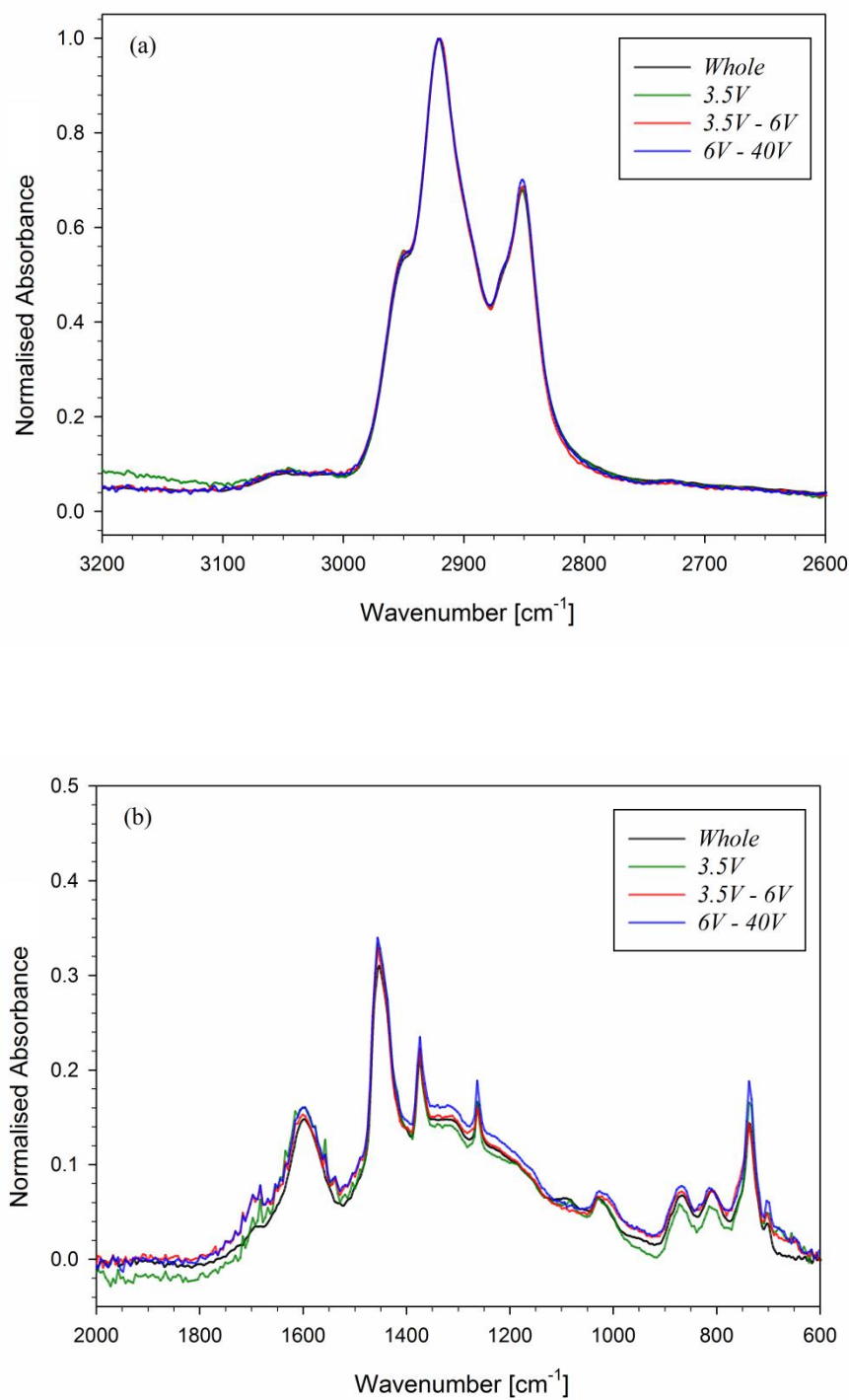
Figure 4: FTIR spectra of asphaltene fractions obtained by stepwise precipitation using n-hexane in the spectral range (a)3200 - 2600 cm^{-1} (b)2000 - 600 cm^{-1}.

The absorbance peaks observed between 2935 - 2915cm^{-1} and 2865 - 2845 cm^{-1} in figure 4(a) correspond to asymmetric and symmetric stretching vibration of methylene groups. All the

asphaltene sub-fractions show similar absorbance in the above spectral range. The spectral region 1760 - 1665 cm^{-1} corresponds to stretching vibrations of carbonyl groups. Figure 4(b) indicates only a minor difference in the intensity of absorbance among the various asphaltene sub-fractions obtained by stepwise precipitation procedure (*3.5V, 3.5V-6V* and *6V-40V*). Also, all the sub-fractions show similar absorbance intensities at 1600 cm^{-1} (which corresponds to C=C aromatic stretching), 1460 cm^{-1} (which corresponds to $-CH_2-$ bending) and 1380 cm^{-1} (which corresponds to $-CH_3$ bending). Similarly, the presence of band at 1030 cm^{-1} is an indication of sulfoxide groups, which could be due to oxidation. Thus FTIR spectrum indicates that the stepwise precipitation procedure has not produced any particular sub-fraction with enhanced or depleted concentration of functional groups. The asphaltene fractionation based on adsorption onto $CaCO_3$ however resulted in sub-fractions with significant differences in absorption intensity at 1700 cm^{-1} as reported in our previous paper[38]. The *irreversibly-adsorbed* asphaltene sub-fraction exhibited the highest absorption intensity at this wavenumber, and is thus considered to have a larger presence of carbonyl, carboxylic acids or derivative groups.

3.3.   Properties

3.3.1.   Precipitation onset by Near Infrared Spectroscopy (NIR)

A typical near infrared spectra obtained during titration of asphaltenes in toluene solution with n-alkane can be found elsewhere[48]. Figure 5 shows the optical density values measured at 1600 nm for solutions of asphaltene sub-fractions in a mixture of toluene and n-hexane.
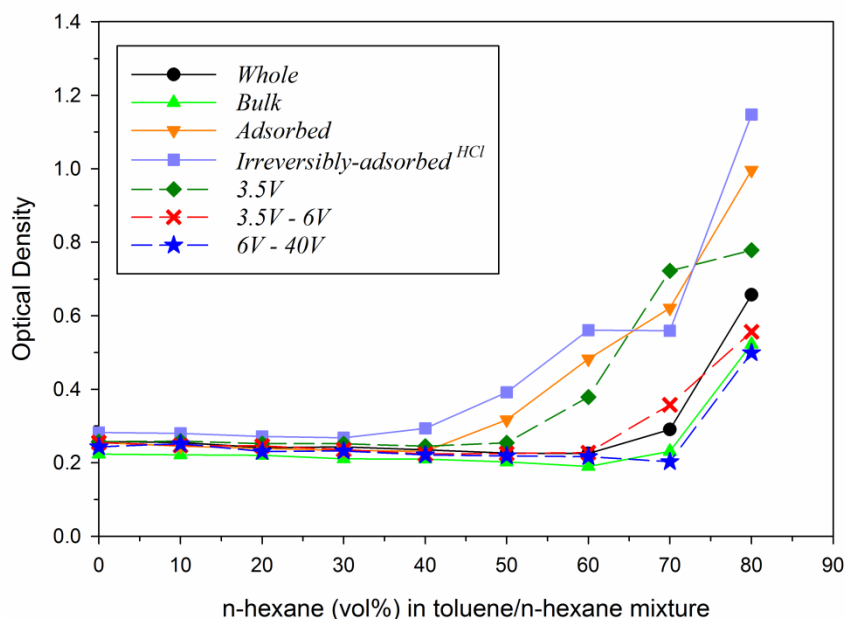
Figure 5: Precipitation of asphaltene sub-fractions in a toluene/n-hexane model system

measured at 1600 nm.

The optical density values in figure 5 correspond to measurements done after 1 hour of n-hexane addition. The values at 1600 nm are reported since this wavelength has minimal hydrocarbon adsorption of NIR light and the optical density measured is mainly due to the scattering of light[14]. The precipitation of asphaltenes leads to scattering of light, and hence the baseline elevation is an indicator of asphaltene precipitation. The solutions were also visually checked using a microscope (Nikon LV 100D) for presence of asphaltene precipitates. The onset of precipitation observed for various asphaltene sub-fractions is given in table 4.

Asphaltene fraction	n-hexane (vol%)
Whole	60 - 70
Bulk	60 - 70

Adsorbed	40 - 50
Irreversibly-adsorbed[HCl]	30 - 40
3.5V	40 - 50
3.5V – 6V	60 - 70
6V – 40V	70 - 80

Table 4: Asphaltene precipitation onset after 1 hr of n-hexane addition

The onset of precipitation of *whole* asphaltenes was between 60-70 vol% n-hexane. Fractionation of asphaltenes based on $CaCO_3$ adsorption showed that the *bulk* asphaltenes exhibit the similar precipitation onset range as the *whole* asphaltenes. However, the *adsorbed* and *irreversibly-adsorbed* asphaltenes precipitate out of the solution on addition of lower amounts of n-hexane. These two asphaltene sub-fractions contain a higher presence of carbonyl, carboxylic acid and derivative groups (based on FTIR) and also a higher concentration of nitrogen heteroatoms than compared to the *bulk* fraction[38]. This suggests that polar and hydrogen bonding interactions may be more dominant in the *adsorbed* and *irreversibly-adsorbed* fractions than compared to *bulk* fraction. Similarly, in the case of asphaltene fractions obtained based on step-wise precipitation method, it was observed that the asphaltene 3.5V fraction has a lower precipitation onset (40-50 vol% n-hexane) than compared to *3.5V - 6V* and *6V - 40V* fractions. This trend is in agreement with the physical principle of separation of these fractions. The higher amount of oxygen in asphaltene *3.5V* indicates that polar interactions and hydrogen bonding could play a more dominant role in this sub-fraction. The solubility characteristics of asphaltene sub-fractions obtained by the two fractionation methods are in agreement with observations of Speicker et al.[11].

3.3.2. Self-association properties by Isothermal Titration Calorimetry (ITC)

The self-association properties of the different asphaltene fractions were determined by injecting 10 g/L asphaltene solutions into the calorimeter cell containing pure xylene. Figure 6 shows a typical plot obtained during the asphaltene deaggregation process followed by ITC. As seen in figure 6(a), the injection of asphaltene solution into xylene results in absorption of heat thereby indicating that the process is endothermic. Dilution results in partial dissociation of physical bonds between asphaltenes which are self-associated. The heat per injection was integrated and values shown in figure 6(b) were obtained after correction for friction heat. It can be observed that the heat absorbed decreases as the asphaltene content in the cell is increased. This is indicative of stepwise association process in asphaltenes and that there is no critical micelle concentration (CMC)[49]. A simple dimer dissociation model (represented in equation 6 and 7) was then used to fit the integrated heat data and obtain the thermodynamic properties.

$$Asp_2 \leftrightarrow Asp + Asp \qquad (6)$$

$$K_{Asp} = \frac{[Asp]^2}{[Asp_2]} \qquad (7)$$

Where Asp and Asp_2 refer to asphaltene monomer and dimer respectively, and K_{Asp} refers to the equilibrium dissociation constant.

The dimer model assumes that asphaltenes exist in the form of dimers and hence deaggregation leads to formation of monomers. The dimer model fit has two fitting parameters: dissociation constant (K_{Asp}) and the enthalpy of dissociation (ΔH_{Asp}). The dimer model has been found to give the best fit for the asphaltene deaggregation process[22, 34].
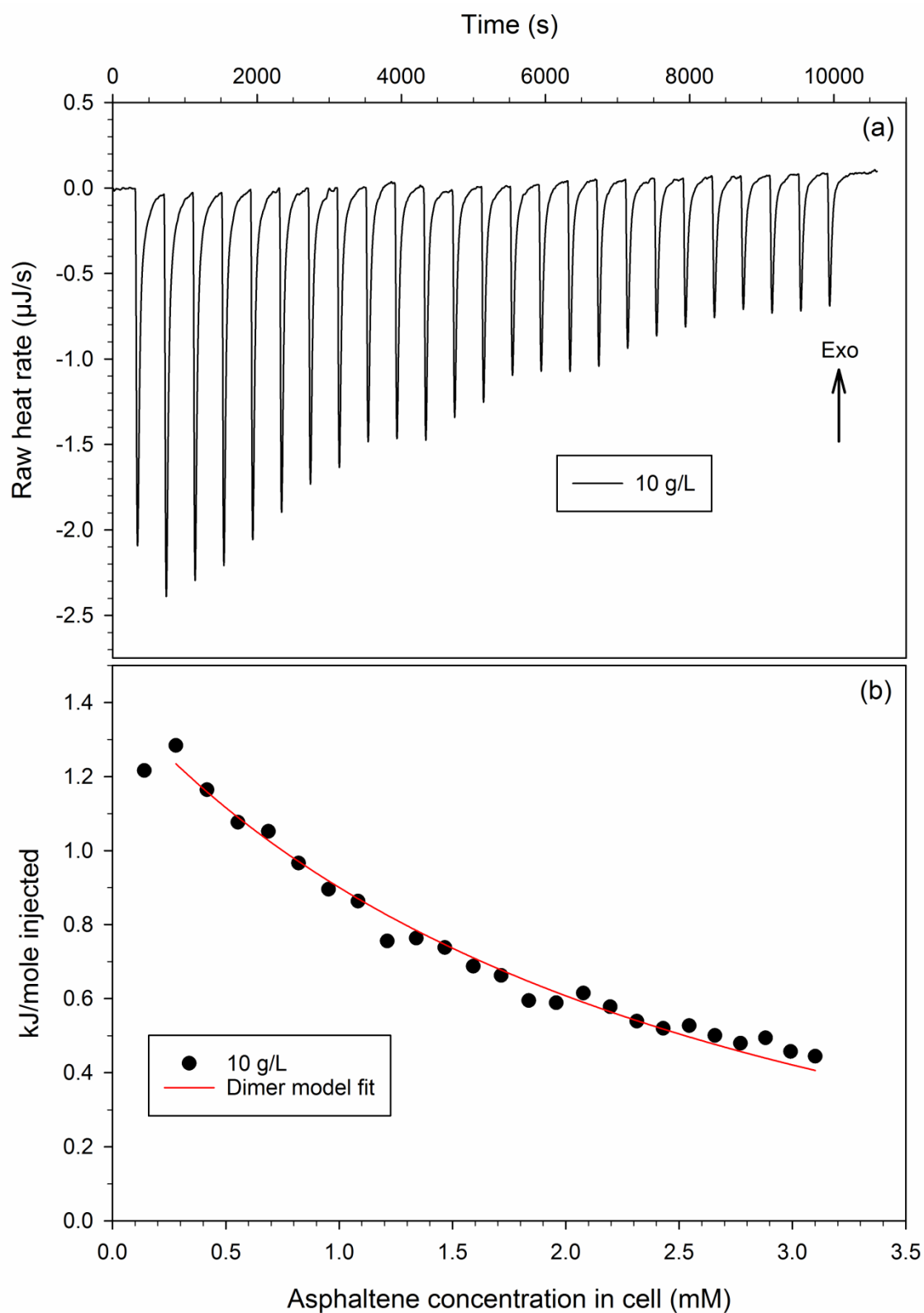
Figure 6: Titration of asphaltenes into xylene. (a) Raw heat data (b) Integrated heat along with dimer dissociation model fit. The heat value from the first injection was discarded for data analysis.

The heat absorbed during titration of various asphaltene sub-fractions is presented in figure 7. Among the asphaltene fractions obtained by adsorption on to CaCO₃, the *irreversibly-adsorbed* asphaltene fraction shows significantly higher heat absorption than compared to *whole*, *bulk* and *adsorbed* asphaltene sub-fractions. The *adsorbed* and *bulk* asphaltene fractions however show slightly lower heat absorption per injection than compared to the *whole* asphaltenes. Similarly, the asphaltene 3.5V sub-fraction shows more heat absorption than compared to *whole*, *3.5V - 6V* and *6V - 40V* asphaltene fractions.
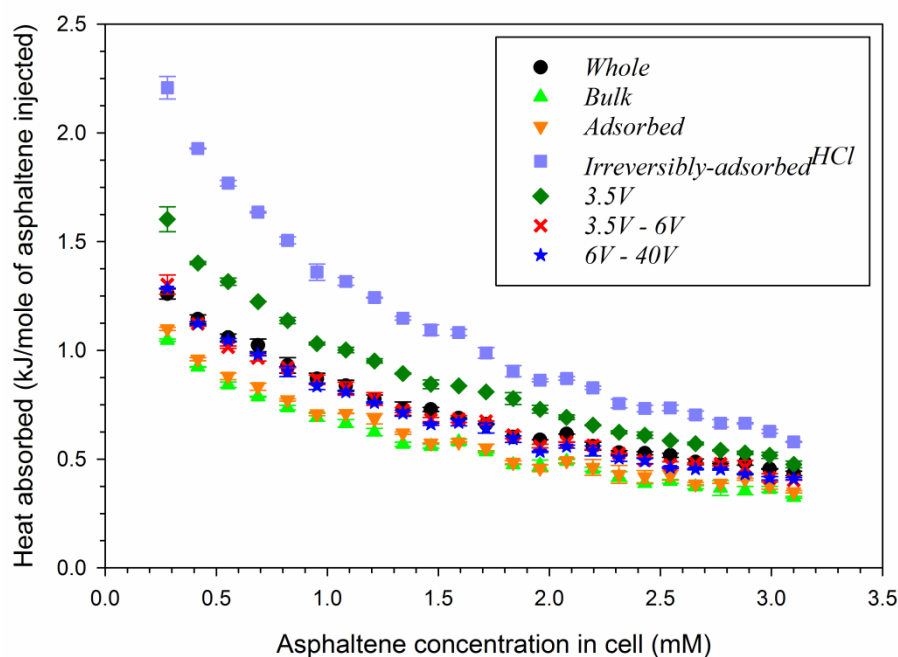

Figure 7: De-aggregation of asphaltene sub-fractions in xylene

The thermodynamic parameters of dimer dissociation model fitting for different asphaltene fractions are given in table 5.

Asphaltene fraction	K_{Asp} (M)	ΔH_{Asp} (kJ/mol)	ΔS_{Asp} (J/molK)
Whole	0.019 ± 0.001	6.1 ± 0.1	53.2 ± 0.5
Bulk	0.019 ± 0.002	4.7 ± 0.1	49.0 ± 0.9
Adsorbed	0.016 ± 0.001	4.8 ± 0.2	50.5 ± 0.6
Irreversibly-adsorbed^{HCl}	0.010 ± 0.001	9.0 ± 0.1	68.3 ± 0.5
3.5V	0.015 ± 0.001	7.1 ± 0.1	58.7 ± 0.4
3.5V – 6V	0.017 ± 0.001	5.8 ± 0.1	53.4 ± 0.1
6V – 40V	0.015 ± 0.001	5.7 ± 0.1	53.9 ± 0.1

Table 5: Thermodynamic parameters of dimer dissociation model fitting

The positive ΔH_{Asp} and ΔS_{Asp} (entropy) values indicate that the process is enthalpy driven. The ΔH_{asp} values obtained for the asphaltene sub-fractions are in the range 4.5 - 9 kJ/mol. The typical Van der Waal interaction strength values are 0.4 – 4 kJ/mol, while those of hydrogen bonds are 12 – 30 kJ/mol[50]. The higher ΔH_{asp} value (9 kJ/mol) for *irreversibly-adsorbed* asphaltenes indicates the presence of stronger bonds in aggregates formed by this sub-fraction. Similarly, the asphaltene *3.5V* fraction has a slightly higher ΔH_{asp} value than *3.5 - 6V* and *6V - 40V* fractions. Both the *3.5V* fraction and the *irreversibly-adsorbed* fractions have a higher presence of heteroatoms which indicates that the more polar asphaltene fractions tend to exhibit a higher tendency to aggregate. The ΔH_{Asp} values were calculated assuming that the molecular weights of all the sub-fractions are 750 g/mol. It must however be noted that the ΔH_{asp} values are sensitive to the molecular weight and hence one must be cautious while interpreting the results based only on the ΔH_{asp} values. The higher heat observed for less soluble asphaltene fractions in the present study is in disagreement with studies by Merino-Garcia & Andersen[34] who observed that the insoluble asphaltene fractions (which was obtained by fractionation of n-heptane precipitated asphaltenes using

mixtures of acetone and toluene) exhibited less heat of dissociation. While the ΔH_{asp} values of asphaltenes fractions in present study are in same order of magnitude as those obtained by Merino-Garcia and Andersen[21], the dissociation constant (K_{asp}) values for asphaltenes fractions in our study are almost 10 times higher. This could be attributed to the difference in origin and composition of asphaltenes.

3.3.3. Aggregate size by DOSY NMR

In the case of dilute systems (0.1 wt% asphaltene solution), we can apply the Stokes-Einstein relation[51] to relate the measured diffusion coefficient to the hydrodynamic radius as follows (equation 8).

$$D_{NMR} = \frac{kT}{6\pi\eta R_H} \quad \leftrightarrow \quad R_H = \frac{kT}{6\pi\eta D_{NMR}} \tag{8}$$

Where D_{NMR} is the measured diffusion coefficient, k is Boltzmann constant, T is absolute temperature η is the viscosity and R_H is the hydrodynamic radius. As the resulting data from a sample of different molecular sizes, an inverse laplace of the experimental data will return a distribution of diffusion coefficients, or as shown in figure 8, a distribution of hydrodynamic sizes.
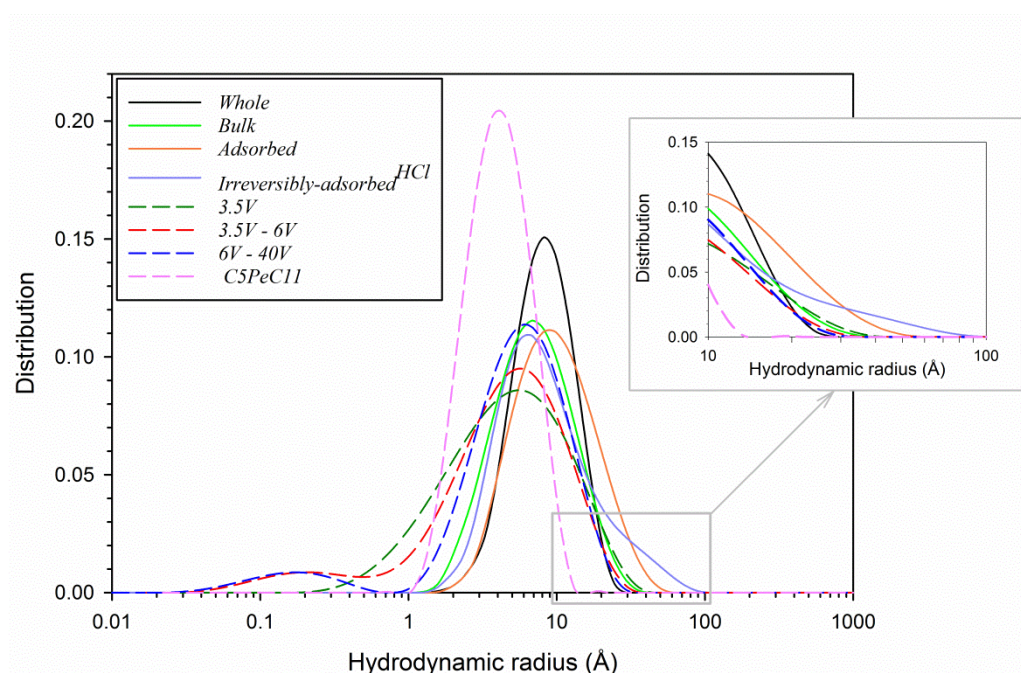
Figure 8: Size distribution of asphaltene fractions and C5PeC11 at 0.1 wt% concentration in

toluene-d8

The average size distribution of all the sub-fractions is summarized in table 6. In the case of

acidic polyaromatic compound C5PeC11, the particle size distribution varies over a narrow

range between 1.3Å and10.2Å, with an average hydrodynamic radius of 4.6Å. This value is

consistent with the existence of C5PeC11 in a mixture of monomers and dimers[52]. The

broader particle size distribution along with a higher average hydrodynamic size for

asphaltene fractions than compared to C5PeC11 indicates that the asphaltene fractions exist

as a mixture of molecular monomers and nanoaggregates. The average hydrodynamic radius

of asphaltene fractions in our study is comparable to the values obtained by Andrews et

al.[53] for coal-derived and petroleum asphaltenes.

Figure 8 shows that the *adsorbed* and *irreversibly-adsorbed* asphaltene fractions have an

ability to form nano-aggregates of large hydrodynamic radius. The *irreversibly-adsorbed*

asphaltenes form nano-aggregates with a size distribution of 1Å - 100Å with an average hydrodynamic radius of 11.2Å. Similarly, the *adsorbed* asphaltenes form nano-aggregates between 1Å and 60Å, with an average hydrodynamic radius of 11.5Å. Both the *adsorbed* and *irreversibly-adsorbed* asphaltenes fractions contain a higher concentration of carbonyl, carboxylic acid or derivate groups compared to other fractions (based on FTIR)[38]. The *bulk* and *whole* asphaltenes however form aggregates of lower size with an average hydrodynamic radius of 8.2Å and 8.9Å respectively. There is one noticeable difference in the size distribution of hydrodynamic radii for asphaltene sub-fractions obtained by the stepwise precipitation method. These sub-fractions (*3.5V, 3.5V - 6V, 6V - 40V*) also show some signal below 1Å. Consequently, the average hydrodynamic radius is lower for these fractions than compared to the fractions obtained by adsorption onto $CaCO_3$. The asphaltene fractions *3.5V – 6V* and *6V – 40V* exhibit a bimodal distribution and show signals below 1Å. Since the shortest carbon-carbon bond length is typically 1.2Å – 1.3Å[54], the origin of signals below 1Å obtained for asphaltene fractions *3.5V – 6V* and *6V – 40V* could be attributed to the impurities.

Asphaltene fraction	Average hydrodynamic radius (Å)
Whole	8.9
Bulk	8.2
Adsorbed	11.5
Irreversibly-adsorbed[HCl]	11.2
3.5V	7.2
3.5V – 6V	6.5

6V – 40V	7.1
C5PeC11	4.6

Table 6: Average NMR hydrodynamic size of asphaltene fractions and C5PeC11

3.3.4. Adsorption onto stainless steel (QCM)

The ability of the *whole*, *bulk*, *adsorbed* and *irreversibly-adsorbed* asphaltene fractions to adsorb on to stainless steel surface has been reported in our earlier publication[38]. The amount of asphaltenes adsorbed on stainless steel (before washing with xylene) followed the order: *irreversibly-adsorbed* ($\sim$ 8 mg/m^2) > *adsorbed* (5.2 $\pm$ 0.3 mg/m^2) > *bulk* (4.4 $\pm$ 0.1 mg/m^2) > *whole* (3.7 $\pm$ 0.1 mg/m^2). The difference in adsorption capability was attributed to the higher presence of carbonic groups, carboxylic acid or their derivative groups. Also, only 15-25 wt% of the asphaltenes desorbed from the stainless steel on washing with xylene[38].

Figure 9 shows the amount of asphaltenes adsorbed onto stainless steel at various asphaltene concentrations in the case of asphaltene fractions obtained by stepwise precipitation procedure. The asphaltene *3.5V* fraction shows the highest adsorption (4.3 $\pm$ 0.1 mg/m^2) onto the stainless steel surface. This fraction has a slightly higher ability to adsorb onto the surface than compared to the *whole* asphaltenes (3.8 $\pm$ 0.1 mg/m^2). In comparison, the *3.5V - 6V* fraction (3.4 $\pm$ 0.2 mg/m^2) and *6V - 40V* fraction (2.9 $\pm$ 0.1 mg/m^2) adsorb to a much lower extent on to stainless steel. The *3.5V* fraction has a significantly higher content of oxygen heteroatoms in it than compared to the other stepwise precipitated fractions. However, all the stepwise precipitated fractions (*whole*, *3.5V*, *3.5V - 6V*, *6V - 40V*) have similar aromaticity (from elemental analysis), aggregate size (based on NMR) and no significant differences in presence of functional groups (based on FTIR analysis). Similarly, only 18 - 28 mass% of the asphaltenes were desorbed from the surface on washing with xylene. The small differences in

composition (based on elemental analysis and FTIR spectra) reported for fractions obtained at different n-hexane/crude oil ratios are in good agreement with QCM data. Indeed the adsorbed amounts vary in a limited range between the asphaltene fractions *3.5V* (4.3 mg/m^2) and *6V - 40V* (2.9 mg/m^2). This behavior is different from the fractions (*bulk*, *adsorbed* and *irreversibly-adsorbed*) obtained by adsorption onto CaCO$_3$, which presented a large difference in their adsorption properties[38].
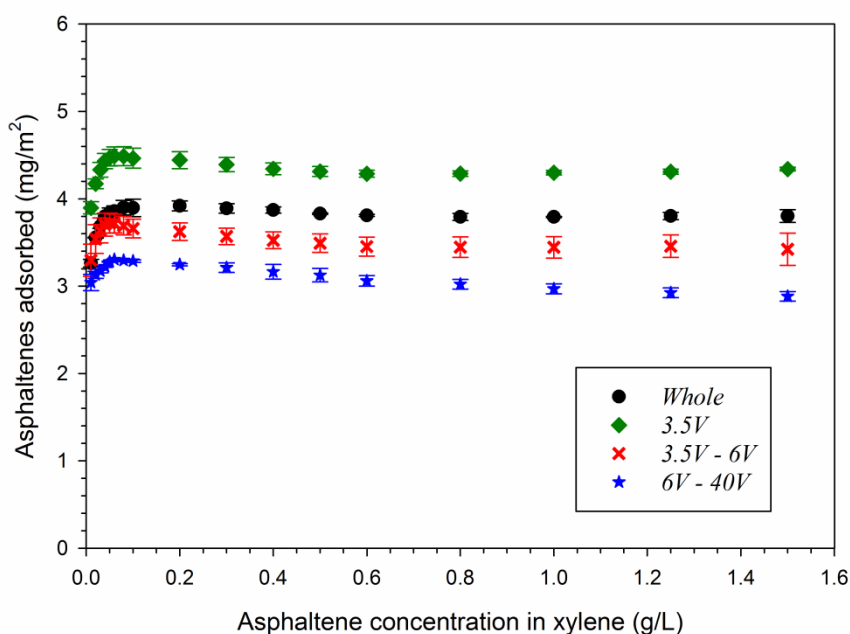

Figure 9: Amount of asphaltenes adsorbed onto stainless steel surface before desorption with xylene.

4.   Comparison of asphaltene fractions obtained by the two fractionation techniques

A comparison of the properties of different asphaltene fractions obtained based on adsorption technique and stepwise precipitation method is given in table 7.

	Asphaltene fractions	
Whole	Based on adsorption on CaCO$_3$	Based on stepwise precipitation

	Bulk	*Adsorbed*	*Irreversibly-adsorbed[HCl]*	*3.5V*	*3.5V-6V*	*6V-40V*
Elemental Analysis:						
Oxygen content (wt%)	1.85	2.33	3.27	4.22	2.84	1.73	1.79
H/C ratio	1.15	1.14	1.14	1.19	1.16	1.14	1.14
Presence of carbonyl, carboxylic acid and derivative groups (FTIR)	-	-	Slightly high	High	Same as *whole* asphaltenes		
Flocculation onset (n-hexane vol%)	60-70%	60-70%	40-50%	30-40%	40-50%	60-70%	70-80%
Self-association properties (ITC)	-	Slightly lower than *whole* asphaltenes	Significantly high	Slightly high	Same as *whole* asphaltenes		
Average hydro-dynamic size in Å (NMR)	8.9	8.2	11.5	11.2	7.2	6.5	7.1
Adsorption on stainless steel in mg/m^2 (QCM)	~ 3.8	~ 4.5	~ 5.3	~ 8	~ 4.3	~ 3.4	~ 2.9

Table 7: Comparison of asphaltene fractions

Fractionation based on adsorption onto $CaCO_3$ has resulted in obtaining asphaltene sub-fractions characterized by significant differences in properties. The properties of the *bulk* asphaltene fraction (which constitutes about 50% of the *whole* asphaltenes) are more representative of the average properties of the *whole* asphaltenes. The asphaltenes were also found consisting of sub-fractions (*adsorbed* and *irreversibly-adsorbed*) that are characterized by a higher presence of functional groups, tendency to form bigger aggregates and exhibiting lower flocculation onset. The observation that larger aggregate size observed for these two sub-fractions leading to an increased tendency to flocculate is in agreement with previous studies[12]. The *adsorbed* and *irreversibly-adsorbed* asphaltene sub-fractions however differ in the aromaticity, oxygen content as well as ability to adsorb onto stainless steel. However, a lower flocculation onset of the *irreversibly-adsorbed* asphaltenes inspite of having a higher H/C ratio (or lower aromaticity) is in contradiction with other studies[12, 13]. The ability of the less aromatic asphaltenes to associate and form larger aggregates have been reported earlier[55]. The *irreversibly-adsorbed* asphaltenes appears to follow this observation, but the *adsorbed* asphaltene fraction contradicts the same. This discrepancy may be due to structural differences between these two fractions. The *irreversibly-adsorbed* asphaltenes are more polar than the *adsorbed* asphaltenes, and hence there exists a possibility of greater influence of specific polar interactions in *irreversibly-adsorbed* asphaltenes in addition to π-π bonding interactions respectively.

In comparison, the stepwise precipitation procedure resulted in asphaltene fractions with fewer differences in structure and properties. The sub-fractions *3.5V – 6V* and *6V – 40V* show similar properties with limited difference mainly in their ability to adsorb onto stainless steel. The asphaltene *3.5V* sub-fraction however has different properties and is characterized by higher oxygen content and slightly enhanced self-association properties (observed in ITC).

The properties of asphaltene *3.5V* fraction have several similarities with the *irreversible-adsorbed* fraction. These two fractions are characterized by higher oxygen content, lower flocculation onset, higher self-association properties (observed by ITC) and a slightly higher ability to adsorb onto stainless steel. However, the asphaltene *3.5V* and *irreversibly-adsorbed* fractions differ in aggregate sizes and the aromaticity. Thus the tendency of asphaltenes to precipitation does not seem to be limited to the solid surface adsorption property.

5.   CONCLUSION

The self-aggregation characteristics for asphaltene sub-fractions obtained from a North Sea crude oil has been investigated using NIR, ITC and DOSY NMR. Asphaltenes were fractionated based on two different techniques: adsorption onto $CaCO_3$ particles and stepwise precipitation from crude oil. The sub-fractions obtained by adsorption of asphaltenes onto $CaCO_3$ showed a significant variation in their characteristics and properties. The less aromatic *irreversibly-adsorbed* asphaltenes fraction, containing more carbonyl, carboxylic acid or derivate groups, showed the highest tendency to self-associate (ΔH_{asp}= 9.0 KJ/mol), formed large aggregates ($\sim$ 11.2 Å) and exhibited a lower flocculation onset (30 - 40 vol% hexane). Similarly, the *adsorbed* asphaltene fraction containing a slightly higher presence of carbonyl groups, formed larger aggregates ($\sim$ 11.5 Å) and had a lower flocculation onset (40 – 50 vol% n-hexane). The *whole* and the *bulk* asphaltenes formed smaller aggregates (8.9 Å and 8.2 Å respectively) and had higher flocculation onset (60 – 70 vol% n-hexane). The *bulk* and *adsorbed* asphaltenes however exhibited a slightly lower ΔH_{asp} than the whole asphaltenes.

On the other hand, only the asphaltene *3.5V* fraction obtained by stepwise precipitation procedure exhibited significantly different properties than *3.5V - 6V* and *6V - 40V* asphaltene

sub-fractions. The asphaltene *3.5V* fraction contained a higher presence of oxygen atoms, exhibited a slightly higher ΔH_{asp} values and had a greater ability to adsorb onto stainless steel than the remaining two fractions. The asphaltene *3.5V* fraction also had a low precipitation onset (40 – 50 vol% n-hexane). The fractions *3.5V - 6V* and *6V - 40V* had a higher flocculation onset (60 - 70 vol% and 70 - 80 vol% n-hexane respectively). The three fractions formed aggregates of similar size.

A comparison of fractions shows that the *irreversibly-adsorbed* asphaltenes and the asphaltene *3.5V* fraction had several similarities in properties including a higher oxygen heteroatom content, higher tendency to aggregate and greater ability to adsorb onto stainless steel surface compared to rest of the fractions. A difference in aromaticity and size of aggregate formed by these two fractions was however observed. Even though these two fractions represent the most polar sub-fractions in the respective fractionation techniques, there appears to be a difference in the nature of interaction present, with the *irreversibly-adsorbed* asphaltenes probably having a higher influence of polar interactions than compared to the asphaltene *3.5V* fraction. The observation that a slightly less polar *adsorbed* asphaltene sub-fraction exhibiting several similar properties as *irreversibly-adsorbed* properties including lower precipitation onset and similar aggregate size despite of having a lower ΔH_{asp} values indicates that the asphaltene precipitation phenomena depends on both the polarity as well as aromaticity.

6.   AUTHOR INFORMATION

Corresponding author

Email address: sreedhar.subramanian@ntnu.no

Tlf: (+47) 73 59 41 59

7. ACKNOWELEDGEMENT

REFERENCES

[1] H.W. Yarranton, Asphaltene Self-Association, Journal of Dispersion Science and Technology, 26 (2005) 5-8.

[2] J. Sjöblom, N. Aske, I. Harald Auflem, Ø. Brandal, T. Erik Havre, Ø. Sæther, A. Westvik, E. Eng Johnsen, H. Kallevik, Our current understanding of water-in-crude oil emulsions.: Recent characterization techniques and high pressure performance, Advances in Colloid and Interface Science, 100–102 (2003) 399-473.

[3] O.C. Mullins, H. Sabbah, J. Eyssautier, A.E. Pomerantz, L. Barré, A.B. Andrews, Y. Ruiz-Morales, F. Mostowfi, R. McFarlane, L. Goual, R. Lepkowicz, T. Cooper, J. Orbulescu, R.M. Leblanc, J. Edwards, R.N. Zare, Advances in Asphaltene Science and the Yen–Mullins Model, Energy & Fuels, 26 (2012) 3986-4003.

[4] H. Sabbah, A.L. Morrow, A.E. Pomerantz, R.N. Zare, Evidence for Island Structures as the Dominant Architecture of Asphaltenes, Energy & Fuels, 25 (2011) 1597-1604.

[5] A. Sharma, H. Groenzin, A. Tomita, O.C. Mullins, Probing Order in Asphaltenes and Aromatic Ring Systems by HRTEM, Energy & Fuels, 16 (2002) 490-496.

[6] A.B. Andrews, J.C. Edwards, A.E. Pomerantz, O.C. Mullins, D. Nordlund, K. Noringa, Comparison of Coal-Derived and Petroleum Asphaltenes by 13C Nuclear Magnetic Resonance, DEPT, and XRS, Energy & Fuels, 25 (2011) 3068-3076.

[7] O.C. Mullins, The Modified Yen Model, Energy & Fuels, 24 (2010) 2179-2207.

[8] J. Murgich, Molecular Simulation and the Aggregation of the Heavy Fractions in Crude Oils, Molecular Simulation, 29 (2003) 451-461.

[9] T. Kuznicki, J.H. Masliyah, S. Bhattacharjee, Molecular Dynamics Study of Model Molecules Resembling Asphaltene-Like Structures in Aqueous Organic Solvent Systems, Energy & Fuels, 22 (2008) 2379-2389.

[10] M.R. Gray, R.R. Tykwinski, J.M. Stryker, X. Tan, Supramolecular Assembly Model for Aggregation of Petroleum Asphaltenes, Energy & Fuels, 25 (2011) 3125-3134.

[11] P.M. Spiecker, K.L. Gawrys, P.K. Kilpatrick, Aggregation and solubility behavior of asphaltenes and their subfractions, Journal of Colloid and Interface Science, 267 (2003) 178-193.

[12] J.-A. Östlund, P. Wattana, M. Nydén, H.S. Fogler, Characterization of fractionated asphaltenes by UV–vis and NMR self-diffusion spectroscopy, Journal of Colloid and Interface Science, 271 (2004) 372-380.

[13] E. Rogel, O. Leon, Y. Espidel, Y. Gonzalez, Asphaltene Stability in Crude Oils, SPE Production and Facilities, 16 (2001) 84-88.

[14] N. Aske, H. Kallevik, E.E. Johnsen, J. Sjöblom, Asphaltene Aggregation from Crude Oils and Model Systems Studied by High-Pressure NIR Spectroscopy, Energy & Fuels, 16 (2002) 1287-1295.

[15] I.H. Auflem, T.E. Havre, J. Sjöblom, Near-IR study on the dispersive effects of amphiphiles and naphthenic acids on asphaltenes in model heptane-toluene mixtures, Colloid and Polymer Science, 280 (2002) 695-700.

[16] D. Espinat, J.C. Ravey, V. Guille, J. Lambard, T. Zemb, J.P. Cotton, Colloidal macrostructure of crude oil studied by neutron and X-ray small angle scattering techniques, Journal De Physique. IV : JP, 3 (1993) 181-184.

[17] M.P. Hoepfner, C. Vilas Bôas Fávero, N. Haji-Akbari, H.S. Fogler, The Fractal Aggregation of Asphaltenes, Langmuir, 29 (2013) 8799-8808.

[18] S. Acevedo, K. Guzman, O. Ocanto, Determination of the Number Average Molecular Mass of Asphaltenes (Mn) Using Their Soluble A2 Fraction and the Vapor Pressure Osmometry (VPO) Technique, Energy & Fuels, 24 (2010) 1809-1812.

[19] H.W. Yarranton, H. Alboudwarej, R. Jakher, Investigation of Asphaltene Association with Vapor Pressure Osmometry and Interfacial Tension Measurements, Industrial & Engineering Chemistry Research, 39 (2000) 2916-2924.

[20] O. León, E. Rogel, J. Espidel, G. Torres, Asphaltenes: Structural Characterization, Self-Association, and Stability Behavior, Energy & Fuels, 14 (2000) 6-10.

[21] D. Merino-Garcia, S.I. Andersen, Isothermal Titration Calorimetry and Fluorescence Spectroscopy Study of Asphaltene Self-Association in Toluene and Interaction with a Model Resin, Petroleum Science and Technology, 21 (2003) 507-525.

[22] D. Wei, E. Orlandi, S. Simon, J. Sjöblom, M. Suurkuusk, Interactions between asphaltenes and alkylbenzene-derived inhibitors investigated by isothermal titration calorimetry, Journal of Thermal Analysis and Calorimetry, 120 (2015) 1835-1846.

[23] D. Merino-Garcia, J. Murgich, S.I. Andersen, Asphaltene Self-Association: Modeling and Effect of Fractionation With A Polar Solvent, Petroleum Science and Technology, 22 (2004) 735-758.

[24] E. Durand, M. Clemancey, A.-A. Quoineaud, J. Verstraete, D. Espinat, J.-M. Lancelin, 1H Diffusion-Ordered Spectroscopy (DOSY) Nuclear Magnetic Resonance (NMR) as a

Powerful Tool for the Analysis of Hydrocarbon Mixtures and Asphaltenes, Energy & Fuels, 22 (2008) 2604-2610.

[25] E. Durand, M. Clemancey, J.-M. Lancelin, J. Verstraete, D. Espinat, A.-A. Quoineaud, Aggregation States of Asphaltenes: Evidence of Two Chemical Behaviors by 1H Diffusion-Ordered Spectroscopy Nuclear Magnetic Resonance, The Journal of Physical Chemistry C, 113 (2009) 16266-16276.

[26] E. Durand, M. Clemancey, J.-M. Lancelin, J. Verstraete, D. Espinat, A.-A. Quoineaud, Effect of Chemical Composition on Asphaltenes Aggregation, Energy & Fuels, 24 (2010) 1051-1062.

[27] N.V. Lisitza, D.E. Freed, P.N. Sen, Y.-Q. Song, Study of Asphaltene Nanoaggregation by Nuclear Magnetic Resonance (NMR)†, Energy & Fuels, 23 (2009) 1189-1193.

[28] K.L. Gawrys, P. Matthew Spiecker, P.K. Kilpatrick, The Role of Asphaltene Solubility and Chemical Composition on Asphaltene Aggregation, Petroleum Science and Technology, 21 (2003) 461-489.

[29] J. Murgich, D. Merino-Garcia, S.I. Andersen, J. Manuel del Río, C.L. Galeana, Molecular Mechanics and Microcalorimetric Investigations of the Effects of Molecular Water on the Aggregation of Asphaltenes in Solutions, Langmuir, 18 (2002) 9080-9086.

[30] D. Merino-Garcia, S.I. Andersen, Thermodynamic Characterization of Asphaltene−Resin Interaction by Microcalorimetry, Langmuir, 20 (2004) 4559-4565.

[31] D. Wei, E. Orlandi, M. Barriet, S. Simon, J. Sjöblom, Aggregation of tetrameric acid in xylene and its interaction with asphaltenes by isothermal titration calorimetry, Journal of Thermal Analysis and Calorimetry, 122 (2015) 463-471.

[32] D. Merino-Garcia, S.I. Andersen, Interaction of Asphaltenes with Nonylphenol by Microcalorimetry, Langmuir, 20 (2004) 1473-1480.

[33] D. Fenistein, L. Barré, Experimental measurement of the mass distribution of petroleum asphaltene aggregates using ultracentrifugation and small-angle X-ray scattering, Fuel, 80 (2001) 283-287.

[34] D. Merino-Garcia, S. Andersen, Application of Isothermal Titration Calorimetry in the Investigation of Asphaltene Association, in: O. Mullins, E. Sheu, A. Hammami, A. Marshall (Eds.) Asphaltenes, Heavy Oils, and Petroleomics, Springer New York2007, pp. 329-352.

[35] J.-A. Östlund, S.-I. Andersson, M. Nydén, Studies of asphaltenes by the use of pulsed-field gradient spin echo NMR, Fuel, 80 (2001) 1529-1533.

[36] H. Kawashima, T. Takanohashi, M. Iino, S. Matsukawa, Determining Asphaltene Aggregation in Solution from Diffusion Coefficients As Determined by Pulsed-Field Gradient Spin−Echo 1H NMR, Energy & Fuels, 22 (2008) 3989-3993.

[37] G. Zheng, W.S. Price, Enviromental NMR: Diffusion Ordered Spectroscopy Methods, in: M.J. Simpson, A.J. Simpson (Eds.) NMR Spectroscopy : A Versatile Tool for Environmental Research, John Wiley & Sons Limited, Sussex, United Kingdom, 2014.

[38] S. Subramanian, S. Simon, B. Gao, J. Sjöblom, Asphaltene fractionation based on adsorption onto calcium carbonate: Part 1. Characterization of sub-fractions and QCM-D measurements, Colloids and Surfaces A: Physicochemical and Engineering Aspects, 495 (2016) 136-148.

[39] D. Pradilla, S. Simon, J. Sjöblom, J. Samaniuk, M. Skrzypiec, J. Vermant, Sorption and Interfacial Rheology Study of Model Asphaltene Compounds, Langmuir, 32 (2016) 2900-2911.

[40] K.F. Morris, C.S. Johnson, Diffusion-ordered two-dimensional nuclear magnetic resonance spectroscopy, Journal of the American Chemical Society, 114 (1992) 3139-3141.

[41] C. Johnson, Diffusion ordered nuclear magnetic resonance spectroscopy: principles and applications, Progress in Nuclear Magnetic Resonance Spectroscopy, 34 (1999) 203-256.

[42] G.H. Sørland, Characterization of Emulsions by PFG-NMR, AIP Conference Proceedings, 1330 (2011) 27-30.

[43] G.H. Sørland, B. Hafskjold, O. Herstad, A stimulated-echo method for diffusion measurements in heterogeneous media using pulsed field gradients, Journal of magnetic resonance, 124 (1997) 172-176.

[44] A. Jerschow, N. Müller, Suppression of convection artifacts in stimulated-echo diffusion experiments. Double-stimulated-echo experiments, Journal of Magnetic Resonance, 125 (1997) 372-375.

[45] G. Sauerbrey, Verwendung von Schwingquarzen zur Wägung dünner Schichten und zur Mikrowägung, Zeitschrift für Physik, 155 (1959) 206-222.

[46] M. Rodahl, F. Höök, A. Krozer, P. Brzezinski, B. Kasemo, Quartz crystal microbalance setup for frequency and Q-factor measurements in gaseous and liquid environments, Review of Scientific Instruments, 66 (1995) 3924-3930.

[47] M. Fossen, H. Kallevik, K.D. Knudsen, J. Sjöblom, Asphaltenes Precipitated by a Two-Step Precipitation Procedure. 2. Physical and Chemical Characteristics, Energy & Fuels, 25 (2011) 3552-3567.

[48] N. Aske, Characterisation of Crude Oil Components, Asphaltene Aggregation and Emulsion Stability by means of Near Infrared Spectroscopy and Multivariate Analysis Department of Chemical Engineering, Norwegian University of Science and Technology (NTNU), Trondheim, 2002.

[49] D. Merino-Garcia, Calorimetric investigations of asphaltene self-association and interaction with resins, in: S.I. Andersen (Ed.) Department of Chemical Engineering Technical University of Denmark, Copenhagen, 2004.

[50] R.H. Garrett, C.M. Grisham, Biochemistry, Fourth ed., Brookes-Cole, Boston, USA, 2008.

[51] A. Einstein, Über die von der molekularkinetischen Theorie der Wärme geforderte Bewegung von in ruhenden Flüssigkeiten suspendierten Teilchen, Annalen der physik, 322 (1905) 549-560.

[52] S. Simon, D. Wei, M. Barriet, J. Sjöblom, An ITC and NMR study of interaction and complexation of asphaltene model compounds in apolar solvent I: Self-association pattern, Colloids and Surfaces A: Physicochemical and Engineering Aspects, 494 (2016) 108-115.

[53] A.B. Andrews, W.-C. Shih, O.C. Mullins, K. Norinaga, Molecular Size Determination of Coal-Derived Asphaltene by Fluorescence Correlation Spectroscopy, Applied Spectroscopy, 65 (2011) 1348-1356.

[54] A.A. Zavitsas, The relation between bond lengths and dissociation energies of carbon-carbon bonds, The Journal of Physical Chemistry A, 107 (2003) 897-898.

[55] H.W. Yarranton, D.P. Ortiz, D.M. Barrera, E.N. Baydak, L. Barré, D. Frot, J. Eyssautier, H. Zeng, Z. Xu, G. Dechaine, M. Becerra, J.M. Shaw, A.M. McKenna, M.M. Mapolelo, C. Bohne, Z. Yang, J. Oake, On the Size Distribution of Self-Associated Asphaltenes, Energy & Fuels, 27 (2013) 5083-5106.